Available online at www.sciencedirect.com
SCIENCE DIRECT
Spectrochimica Acta Part A 64 (2006) 338–342
SPECTROCHIMICA ACTA PART A
www.elsevier.com/locate/saa

Near-infrared diode laser wavelength modulation-based photoacoustic spectrometer

Jingsong Li *, Xiaoming Gao, Weizheng Li, Zhensong Cao, Lunhua Deng, Weixiong Zhao, Mingqiang Huang, Weijun Zhang

Environmental Spectroscopy Laboratory, Anhui Institute of Optics & Fine Mechanics, Chinese Academy Sciences, P.O. Box 1125, Hefei 230031, PR China

Received 8 June 2005; received in revised form 8 July 2005; accepted 14 July 2005

Abstract

An inexpensive resonant photoacoustic spectrometer based on a low-power distributed feedback diode laser and wavelength modulation spectroscopy is developed. This sensor has been applied to the detection of acetylene (C_2H_2) using a properly designed photoacoustic cell operating on its second longitudinal mode. The minimum detectable limit of about 10 parts-per-million volume (signal to noise ratio = 1) is achieved at atmospheric pressure, and the pressure and laser power linear dependence of the photoacoustic signal is also investigated. Moreover, in this paper we also describe some basic theory of gas photoacoustic spectroscopy.
© 2005 Elsevier B.V. All rights reserved.

Keywords: Photoacoustic spectroscopy; DFB diode laser; Wavelength modulation; C_2H_2

1. Introduction

Laser photoacoustic spectroscopy (LPAS) has been used as a very sensitive spectroscopic technique in trace gas detection and analysis, such as environmental monitoring, industrial process control, automotive exhaust analysis, agricultural monitoring and medical diagnostics [1]. Since the photoacoustic signal is proportional to the power of the laser light through the PA cell, early photoacoustic spectra researches use high intense CO and CO_2 lasers in the mid-infrared [2–5] as light sources. However, these light sources are only line tunable, thus the laser and measured molecular absorption lines must coincide with each other for good sensitivity. Lately, transportable PA spectrometers based on cw-ICLs and cw-OPOs have been developed. Both laser systems are sensitive and selective, but expensive and comparatively complicated in setup [6,7]. Recently, with tunable diode laser developing, room operating diode lasers, have fast respond and wavelength modulation, are used in photoacoustic spectroscopy [8,9]. As it is known, often window and wall background PA signals limit the sensitivity of the PA detection system. In wavelength modulation spectroscopy the laser frequency is modulated with f, but the PA signals are analyzed at the frequency $2f$. This can reduce the effect of these background noises on the detection sensitivity [10–12].

Acetylene is a well-known industrial gas. It is the lowest molecular weight analog of the class of neutral organic, acetylenic compounds. This substance is also known as ethyne. Acetylene is a gas that forms highly explosive mixtures in air across a broad range of concentrations. The lower explosive limit is 2.5% in air (National Fire Protection Association, 1997). Moreover, as a characteristic gas, acetylene is usually analyzed in dissolved gas-in-oil analysis to diagnose the potential inner faults of power transformers [13]. Owing to its flammability and explosivity, the monitoring and analysis of acetylene at low concentration has become an essential environmental and industrial issue.

In this paper, a portable, low cost, simple, highly sensitive photoacoustic spectrometer based on diode laser modulation spectroscopy was developed. A near-infrared distributed-feedback (DFB) laser diode at 1511.51 nm is used in order to excite the R25 rotational line of the $101000+u<-000000+g$ vibrational C_2H_2

* Corresponding author. Tel.: +86 551 5593174; fax: +86 551 5591551.
E-mail address: ljs0625@126.com (J. Li).

1386-1425/$ – see front matter © 2005 Elsevier B.V. All rights reserved.
doi:10.1016/j.saa.2005.07.029

transition (absorption line $\nu = 6608.5124\,\mathrm{cm}^{-1}$ and intensity $S = 1.414\mathrm{E}{-}21\,\mathrm{cm}^{-1}/(\mathrm{molecule\,cm}^{-2})$), which was selected for the experiment on the basis of laser availability. The realization of our system is described and experimental results are presented.

2. Theory of laser PAS

PAS is a calorimetric spectroscopy technique based on the photoacoustic effect, and has gradually matured in utility since its discovery by Bell in 1880 [14,15] with significant performance improvements in light sources and modulators, in wavelength tunability, and in photoacoustic signal transducers. The generation and detection of the PA signal in a gaseous sample consists of four main steps [16]:

- Molecular absorption of electromagnetic radiation, resulting in an excitation of the absorbing molecules to a high energy level (electronic, vibrational or rotational quantum state).
- Nonradiative relaxation of the excited state (collosional relaxation), the optical energy previously absorbed is completely or partly released as heat in the sample, thus, giving rise to the temperature increase of the gas due to the energy transfer to translation, resulting in an increase of the gas pressure.
- When the laser intensity is modulated at an acoustic frequency, the temperature changes periodically, and so does the pressure, which can be observed as an acoustic signal.
- Detection of the acoustic signal using a sensitive microphone.

If we neglect the influence of the thermal and the viscous interaction of the gas, the wave equation of the acoustic pressure changes p is [17]:

$$\nabla^2 p(\vec{r},t) - \frac{1}{c^2}\frac{\partial^2 p(\vec{r},t)}{\partial t} = -\frac{\gamma - 1}{c^2}\frac{\partial H(\vec{r},t)}{\partial t} \tag{1}$$

where c is the speed of sound in the given gas, $H(\vec{r},t)$ represents the heat sources produced by the absorption of the laser light and Υ is the ratio of the specific heats $C_\mathrm{P}/C_\mathrm{V}$ of the studied gas at constant pressure and constant volume. In the case of small absorptions ($\alpha \ll 1$), the deposited heat energy $H(\vec{r},t)$ is directly proportional to the molecular absorption coefficient α and to the laser beam intensity $I(\vec{r},t) = I_0(\vec{r},t)\,\mathrm{e}^{\mathrm{i}\omega t}$:

$$H(\vec{r},t) = \alpha I(\vec{r},t) \tag{2}$$

The solution of the inhomogeneous wave Eq. (1) is described by the eigenfunction series:

$$p(\vec{r},t) = \sum_j A_j(t)\,p_j(\vec{r})\exp(\mathrm{i}\omega_j t) \tag{3}$$

where $P_j(\vec{r})$ are the eigensolutions and $A_j(t)$ describes the time-dependent amplitudes of the different modes. The eigensolutions for a cell with the shape of cylinder with radius R and length L in cylindrical coordinates $[\vec{r} = (r,\varphi,z)]$ are described by

$$p_j(\vec{r}) = J_m\left(\frac{\pi\alpha_{mn}}{R}r\right)\cos\left(\frac{k\pi}{L}z\right)\left[\begin{matrix}\sin\\ \cos\end{matrix}(m\varphi)\right] \tag{4}$$

where J_m are the Bessel functions of the series m, and α_{mn} is the nth zero of the first derivative of the mth Bessel function divided by π, whose first values are given in Table 1. Every mode j is characterized by three numbers $j = (n,m,k)$, Ref. to Fig. 1, corresponding to radial, azimuthal and longitudinal contributions to the given mode, respectively. The frequency of the jth eigenmode can be determined from the relationship:

$$f_j = f_{nmk} = \frac{\omega_j}{2\pi} = \frac{c}{2}\sqrt{\left(\frac{\alpha_{mn}}{R}\right)^2 + \left(\frac{k}{L}\right)^2} \tag{5}$$

The resonance frequency is directly proportional to the sound velocity, which can be described as [18]:

$$c = \sqrt{\frac{\gamma RT}{M}} \tag{6}$$

where $R = 8.314\,\mathrm{J(mol\,K)}^{-1}$ is the constant of perfect gases, M the molar mass of the gas, and T is the temperature. Some physical constants are usually different between different buffer gases. The values of this parameters are listed in Table 2 for N_2 gas.

Table 1
Numerical values of the parameters α_{mn} for the first derivative of cylindrical Bessel functions

α_{mn}	n			
m	0	1	2	3
0	0	1.21976	2.23326	3.23817
1	0.58601	1.69691	2.71709	3.72645
2	0.97212	2.13459	3.17323	4.19214
3	1.33722	2.55125	3.61154	4.64287

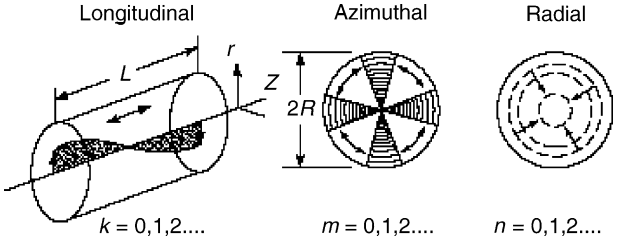

Fig. 1. Resonant acoustic modes of a cylindrical closed chamber; the fundamental longitudinal, azimuthal and radial modes.

Table 2
Physical constants of N_2 buffer gas at 20 °C and 1 atm

Substance	γ	M (kg mol^{-1})	c (m/s)
N_2	1.401	0.028	349

In addition, these modes are orthogonal and can be normalized by the condition:

$$\int p_i p_j^* \, \mathrm{d}V = V_c \delta_{ij} \tag{7}$$

where the integration is carried out across the entire volume of the photoacoustic cell, $V = \pi R^2 L$ is the cell volume and δ_{ij} is the Dirac delta function.

Combination of relationships upwards, The amplitude of mode j is given by

$$A_j(\omega) = -\frac{\mathrm{i}\omega}{\omega_j^2} \frac{\alpha[(\gamma - 1)/V_c] \int_{V_c} p_j^* I \, \mathrm{d}V}{(1 - \omega^2/\omega_j^2 - i\omega/\omega_j Q_j)} \tag{8}$$

where Q_j is the quality factor of the resonance, usually defined as the ratio between the resonance and the frequency bandwidth at $1/\sqrt{2}$ of the maximum, that takes into account the losses in the acoustic wave. The integral in the numerator of the expression of the mode amplitude $A_j(\omega)$ represents the coupling between the laser beam profile and the acoustic mode. Therefore, effective coupling between the laser beam distribution and the acoustic mode results in an efficient excitation of the maximize PA signal.

3. PAS sensing system

Our PA measuring system is shown schematically in Fig. 2. The room-temperature single mode distributed feedback (DFB) diode laser is fibre-coupled and the optical fibre ends with a beam collimator, and the laser beam is aligned on the cylindrical sample cell axis. The stainless steel PA cell consists of two buffer volumes (about half the length of the resonator) sealed with Brewster-angled windows and a central cylindrical resonator ($L = 15$ cm, $R = 1.5$ cm) designed to be operated in its second longitudinal mode. The Brewster windows are made of SiO_2 with a thickness of 3 mm. The miniature electret microphone (Institute of Acoustics, The Chinese Academy of Sciences, Mode MA211, sensitivity 50 mV/Pa) was placed in the centre (on the wall) of the resonator.

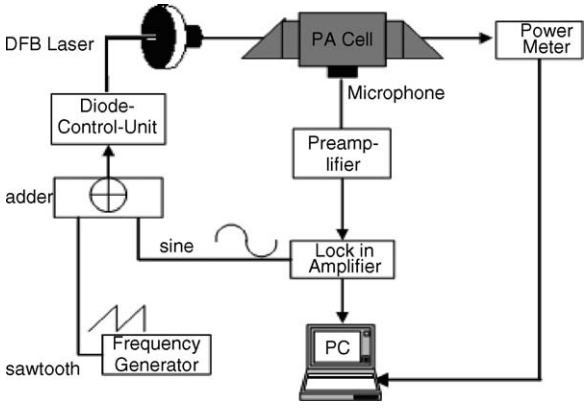

Fig. 2. Experimental arrangement for the photoacoustic measurements.

The added signals of sawtooth-wave from function generator (GW, Model GFG-8019G) and sine-wave from digital lock-in amplifier (Stanford Research Systems, Mode SR830) by home-made adder were used to modulate current of the diode laser by the commercial diode laser controller (ILX Lightwave LDX-3724, current stability 0.005%, temperature stability ≈0.01%). The microphone signal, amplified by a factor of 100 (EG&G, Model 5113) with a bandpass filter set at 30 Hz–30 kHz, was sent to lock-in amplifier, with a time constant usually set to 1ms, and ultimately acquired by the LabWindows/CVI-controlled data gathering and processing system with a sampling frequency and total number of samples of 20 kHz and 8192, respectively. By setting a center current of 70 mA and an operational temperature of 44.1 °C, the laser was wavelength modualated to scan over the R25 absorption line of C_2H_2 by tuning the current of the laser from 50 to 90 mA with sawtooth-wave (amplitude: 1 V, frequency: 0.8 Hz) and sine-wave (amplitude: 114 mV, frequency: 1.05 kHz). This results in a mode-hop free scan from 6608.0 to 6609.0 cm^{-1}. The modulation depth (0.15 cm^{-1}) was chosen to be one time the absorption line width (FWHM) at 1 atm pressure. A maximum laser output power of 20 mW at 25.01 °C was certified by the manufacturer. However, for the temperature setting used in these experiments (44.1 °C) and fibre-coupled wastage, the mean unmodulated output power measured behind the PA cell by an optical power meter (Newport, Model 1830-C) was 3.5 mW. Dividing the PA signal by the laser power results in a normalized PA signal, which is a measure for the concentration of the absorbing trace gas in the air sample.

4. Results and discussion

4.1. Frequency characteristics and sensitivity of detection

For the resonance PA cell, the resonance frequency (typically 1–4 kHz) mainly depends on two important factors, the cell geometry and the gas mixture inside the cell. For the second longitudinal mode, the resonance frequency is calculated to be about equal to 2.3 kHz for a sound velocity $c_0 = 349$ m/s. However the experimental value of the resonance frequency is 2.1 kHz with a quality factor of $Q = 22$. The discrepancy between theoretical and experimental value may be caused by drifts of the gas temperature. In addition, the surface and volume effects are also not avoided. Main surface losses are thermal and viscous losses of the sound wave at the resonator surface, microphone losses and acoustic wave scattering losses at obstacles in the cell. Volumetric losses are not as important as surface losses and mainly due to free space viscous and thermal losses and V-V, V-R, V-T relaxation losses of ployatomic gas [19]. As we all know, the laser current modulation will cause small modulation of amplitude synchronously. Both wavelength

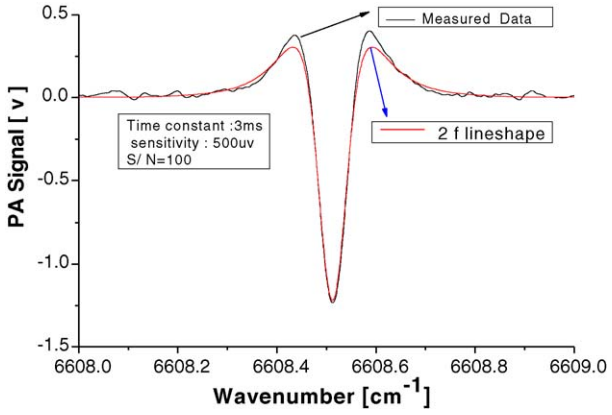

Fig. 3. Measured 2*f* PA spectrum of 0.1% C_2H_2 buffered with N_2 at atmospheric pressure, modulation frequency 1.05 kHz, and fitting according to Ref. [21].

and power changes will influence the PA signal, however, the two effects cannot be separated in the lock-in output signal. If the gas temperature is monitored simultaneously and used to proofread the modulation frequency, the PA signal will be improved. All the measurements performed were at rest, the PA cell was filled with the measured gas, and sealed with valves. Fig. 3 gives an example of the measured PA 2*f* spectrum and the result of fitting. Corresponding to Ref. [20], the calculated signal to noise ratio (SNR) is approximately 100, this SNR indicates that the noise-limited minimal detection limit for this sensor is about 10 ppm V of acetylene.

4.2. Dependence of PA signal on laser power and C_2H_2 concentration

The PA signal is described mathematically:

$$S = S_m PCN_{tot}c_m\sigma \quad (9)$$

where the microphone sensitivity, S_m, is in units of millivolts per Pascal (mV/Pa); the laser optical power, P is in watts (W), the PA cell response constant, C, has units of Pasacl per inverse centimeters per watt (Pa/cm^{-1} W), N_{tot} is the total number density of molecules (molecule/cm^3), and c_m and σ are the concentration and absorption cross section of the analyte, respectively. The PA signal is therefore proportional to the incident laser power and the concentration of the absorbing molecule. Thus, PA detection of trace gases derives sensitivity benefit from the use of as much laser power as is available. Fig. 4 shows the dependence of PA signal on laser power. A linear dependence of PA signal on the DFB laser power was found in the range from 0.5 to 4 mW at constant 1% C_2H_2 concentration. Linear regression leads to an equation of $y = 0.29671x - 0.02449$ with a regression coefficient of $R = 0.99878$ for $n = 9$ samples. The dependence of the PA signal on C_2H_2 concentration between 0.5 and 10.5 Torr buffered with N_2 at 760 Torr pressure is also shown in Fig. 5.

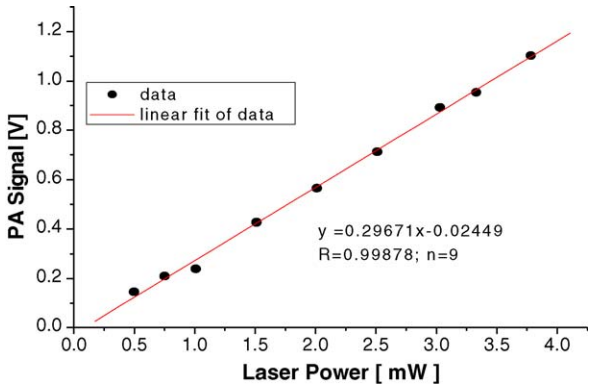

Fig. 4. Dependence of PA signal on the DFB laser power at constant 1% C_2H_2 concentration buffered in N_2.

The linear equation is $y = 0.18251x - 0.00746$ with a regression coefficient of $R = 0.9966$ for $n = 5$ sample points. The results proved that our measurements are consistent with the theoretical results in substance.

While it is not the purpose of this paper to review previous results, some comparison of our system with theirs may be insightful. In Ref. [22], the detection limit of 300 ppm V for C_2H_2 is reported at a pressure of 120 Torr (largest response) with almost the same other experimental conditions except the resonator. In contrast to the results (the minimum detectable absorption coefficient $\alpha_{min} \approx 10^{-9}$ cm^{-1}) presented in Ref. [23] it should be mentioned that they combine the photoacoustic with a multipass configuration (number of reflections: $N = 50$), NaCl-OH$^-$ colour centre laser at 1.5 μm power is 250 mW, and the results obtained are also in the optimal pressure region, not at the atmospheric pressure. The outstanding performance of our PA sensing system is satisfying from comparative results for a low-power near-IR diode laser. However, the sensitivity needs to be further improved for practical applications and other needs. The noises in our system are mainly ambient noise and electrical noise, e.g., circuit noise and intrinsic noise of the microphone and preamplifier. So, if we can eliminate these noises furthermore, the sensitivity will be achieved in the range of several ppb or sub-ppb.

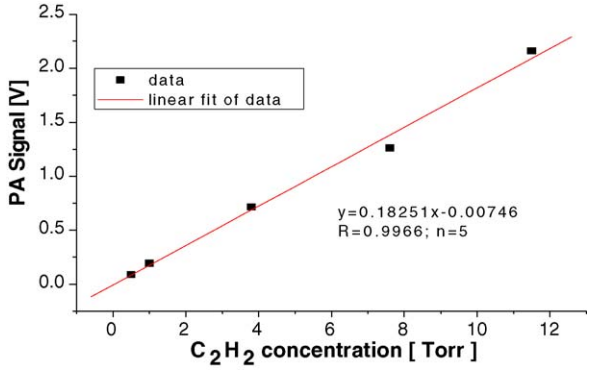

Fig. 5. Concentration dependence of PA signal intensity in 2*f* for C_2H_2.

5. Conclusions

A simple, portable, low cost resonant photoacoustic spectrometer based on near-IR diode laser is reported. Combination of wavelength modulation and PA detection completely eliminates background drifts and fluctuations. The achieved sensitivity is 10 ppm V for acetylene at atmosperic pressure (SNR = 1). The system performances are below expectation for the moment, as a result of some high noise level, but also to the weak optical power launched into the PA cell. It seems likely that further increases in sensitivity could be achieved by protecting the PA cell from outside acoustic and electric interferences. Other ways of achieving high sensitivity are the combination of the photoacoustic with a multipass configuration and differential Helmholtz resonantor [24–28]. The sensitivity can also be improved by increasing the laser power using a high-powered fiber amplifier in the near infrared for low-power DFB diode laser. These improvements should allow to increase appreciably the system performances. These methods will all be considered for improving the sensitivity of our PA system in our future work.

Acknowledgements

This research was funded by the National High Technology Research and Development Program of China grant NO. 2002AA825100 and Natural Science Fund of Anhui Province of China.

References

[1] A. Rosencwaig, Photoacoustics and Photoacoustic Spectroscopy, Science Press, 1980.
[2] Edjar M. Telles, Edson Bezerra, Artemio Scalabrin, Proc. SPIE 4419 (2001) 422–426.
[3] Shaocheng Li, Qingxu Yu, Zhibin Chen, Junxiu Liu, Proc. SPIE 4223 (2000) 145–148.
[4] Ljubica T. Petkovska, Milan S. Trtica, Milovan M. Stoiljkovic, Gordana S. Ristic, Ščepan S. Miljanic, Quant J. Spectrosc. Radiat. Transfer 54 (3) (1995) 509–520.
[5] S. Bernegger, M.W. Sigrist, Infrared Phys. 30 (1990) 375–429.
[6] M. Horstjann, Y.A. Bakhirkin, A.A. Kosterev, R.F. Curl, F.K. Tittel, C.M. Wong, C.J. Hill, R.Q. Yang, Appl. Phys. B 79 (2004) 799–803.
[7] Frank Müller, Alexander Popp, Frank Kühnemann, Stephan Schiller, Opt. Express 11 (22) (2003) 2820–2825.
[8] Anatoliy A. Kosterev, Frank K. Tittle, Appl. Opt. 43 (2004) 6213–6217.
[9] M. Wol, H. Harde, Infrared Phys. Technol. 41 (2000) 283–286.
[10] S. Schäfer, M. Mashni, J. Sneider, A. Mikl'os, P. Hess, H. Pitz, K.-U. Pleban, V. Ebert, Appl. Phys. B 66 (1998) 511–516.
[11] András Miklós, Miklós Fehér, Infrared Phys. Technol. 37 (1996) 21–27.
[12] Miklós Fehér, Yuan Jiang, John P. Maier, András Miklós, Appl. Opt. 33 (9) (1994) 1655–1658.
[13] Liu Xian Yong, Proc. SPIE 5633 (2002) 356–362.
[14] A.G. Bell, Am. J. Sci. 20 (1880) 305–324.
[15] A.G. Bell, Philos. Mag. 11 (5) (1881) 510.
[16] Stéphane Schilt, Luc Thévenaz, Marc Niklès, Lukas Emmenegger, Christoph Hüglin, Spectrochim. Acta Part A 60 (2004) 3259–3268.
[17] Q.R. Yin, T. Wang, M.L. Qian, Photoacoustic and Photothernal Technique and Applications, Science Press, 1991.
[18] Jean-Philippe Besson, Stéphane Schilt, Luc Thévenaz, Spectrochim. Acta Part A 60 (2004) 3449–3456.
[19] A. Karbach, P. Hess, J. Chem. Phys. 83 (1985) 1075–1084.
[20] Michael E. Webber, Michael B. Pushkarsky, C. Kumar, N. Patel, Proc. SPIE 4817 (2002) 111–122.
[21] Xiaoming Gao, Wei Huang, Ziyao Li, Li Fang, Weijun Zhang, Acta Opt. Sin. 23 (5) (2003) 609–611.
[22] P. Kania, S. Civiš, Spectrochim. Acta Part A 59 (2003) 3063–3074.
[23] Ch. Hornberger, M. König, S.B. Rai, W. Demtröder, Chem. Phys. 190 (1995) 171–177.
[24] M. Nägele, M.W. Sigrist, Appl. Phys. B 70 (2000) 895–901.
[25] M.W. Sigrist, A. Bohren, I.G. Calasso, M. Nägele, A. Romann, M. Seiter, Proc. SPIE 4063 (2000) 17–25.
[26] K. Song, H.K. Cha, V.A. Kapitanov, Yu.N. Ponomarev, A.P. Rostov, D. Courtois, B. Parvitte, V. Zeninari, Appl. Phys. B 75 (2002) 215–227.
[27] V. Zeninari, V.A. Kapitanov, D. Courtois, Yu.N. Ponomarev, Infrared Phys. Technol. 40 (1999) 1–23.
[28] Kyuseok Song, Seokwon Oh, Euo Chang Jung, Deokhyun Kim, Hyungki Cha, Microchem. J. 80 (2005) 113–119.